



---

# Geotechnical Testing Journal

---

Hauke Anbergen,<sup>1,2</sup> Jens Frank,<sup>2</sup> Lutz Müller,<sup>3</sup> and Ingo Sass<sup>4</sup>

**DOI: 10.1520/GTJ20130072**

Freeze-Thaw-Cycles on  
Borehole Heat Exchanger  
Grouts: Impact on the  
Hydraulic Properties

---

VOL. 37 / NO. 4 / MONTH 2014



Hauke Anbergen,<sup>1,2</sup> Jens Frank,<sup>2</sup> Lutz Müller,<sup>3</sup> and Ingo Sass<sup>4</sup>

## Freeze-Thaw-Cycles on Borehole Heat Exchanger Grouts: Impact on the Hydraulic Properties

### Reference

Anbergen, Hauke, Frank, Jens, Müller, Lutz, and Sass, Ingo, "Freeze-Thaw-Cycles on Borehole Heat Exchanger Grouts: Impact on the Hydraulic Properties," *Geotechnical Testing Journal*, Vol. 37, No. 4, 2014, pp. 1-13, doi:10.1520/GTJ20130072. ISSN 0149-6115

### ABSTRACT

In this paper a testing device is described that measures the hydraulic conductivity of grout specimens for Borehole Heat Exchangers (BHE). During the operation of closed-loop ground source heat pumps running with antifreeze, freezing of the backfill can occur due to extensive heat extraction. This laboratory device can assess the influence of frost on the hydraulic seals of BHEs. The device is based on a triaxial flexible wall permeameter. A freely selectable number of cyclic freeze-thaw-stresses as well as a confining pressure simulating radial earth pressure ( $\sigma_2 = \sigma_3$ ) can be applied. Specimens are composed of an annular grout body and a polyethylene pipe simulating the BHE system. The freezing direction is perpendicular to the vertical axis of the BHE from the inside to the outside. Numerical coupled modeling was applied to verify the results of the temperature distribution inside the specimens. It was observed and modeled that the propagation of the frost front and the fabric disintegration processes are correlated. Results of three different grouting materials will be presented. With its relative small dimensions the device can be easily implemented into soil mechanical laboratories and thus can contribute to quality control of grouts.

### Keywords

grout material, laboratory test, borehole heat exchanger, flexible wall permeameter, freeze-thaw-cycle, hydraulic conductivity

### Introduction

Shallow geothermal systems can provide an efficient energy source to provide domestic heating and cooling. Especially for decentralized energy supplies, ground coupled heat pump systems can

Ansichtsexemplar. Keine Vervielfältigung erlaubt.

Manuscript received April 17, 2013; accepted for publication February 10, 2014; published online xx xx xxxx.

<sup>1</sup> Chair of Geothermal Science and Technology, Technische Univ. Darmstadt, 64289 Darmstadt, Germany, e-mail: anbergen@geo.tu-darmstadt.de

<sup>2</sup> Frank GeoConsult GmbH, 22085 Hamburg, Germany.

<sup>3</sup> Chair of Geotechnics and Geothermal Science, Hochschule Ostwestfalen-Lippe, Lemgo, Germany.

<sup>4</sup> Chair of Geothermal Science and Technology, Technische Univ. Darmstadt, 64289 Darmstadt, Germany.

be an alternative to common electrical heating/cooling or fossil fuels. Most ground coupled heat pumps in Europe are executed with Borehole Heat Exchangers (BHEs).

As drinking water is often supplied by shallow aquifers, in most European countries it is mandatory to prevent erosion of the backfill inside the borehole or any eventual contamination of the groundwater. Borehole heat exchangers that penetrate aquifers and aquicludes need to be sealed (Allan 2000; Mehnert 2004). The sealing of penetrated aquicludes has to be guaranteed in order to prevent unwanted connections of aquifers. For example, the determining directive for BHEs in Germany, the VDI-4640 of the Association of German Engineers (Verein Deutscher Ingenieure—VDI), prescribes that all BHEs have to be sealed by a grouting material.

Grouting materials have to meet two main requirements:

1. *Securing the heat transport from the rock to the heat carrier fluid during heat extraction or vice versa for heat injection;*
2. *Sealing the borehole to the surface to prevent contaminants from entering the borehole and to seal aquifers that have been penetrated (VDI 2001).*

From the point of view of approval authorities, the first requirement is desirable; the second requirement is essential. The impermeability (or acceptable low permeability) of the system has to be provided under all possible operating conditions.

For an optimized design of a BHE it is necessary to consider accurate parameters like thermal conductivity of the soils penetrated by the borehole. These parameters can be estimated using in situ tests like the geothermal response test (GRT) or enhanced geothermal response test (EGRT). Consequently, the amount of thermal energy that can be supplied by the BHE can be calculated precisely and thus the whole system can be optimized.

An optimized system means that long-term sufficient temperature extraction is guaranteed. If the BHE is used for heating only, it is likely that the soil temperature will decrease in the vicinity of the borehole, especially at the end of heating periods. In order to provide a sufficient heat extraction, the heat pump will run with relatively low working fluid temperatures. Using water as the working fluid restricts the temperature of the return flow from the heat pump to the BHE. To cover peak heating demands during times of extensive heat extraction, national directives (e.g., VDI 2001) permit working fluid temperatures below 0.0°C (32.0°F). Therefore, it is necessary to use working fluids that remain in liquid phase at temperatures below 0.0°C (e.g., monoethyleneglycol-water mixtures) (Mehnert 2004). Consequently, freezing of the surrounding grout or even of surrounding soil is possible (Anbergen and Sass 2013). This process is commonly referred to as freeze-thaw-cycle (FTC).

An undersized borehole length, incorrect parameters from the GRT, or an increase in heating energy demand, which was not considered designing the specific system, may lead to lower working fluid temperatures at higher intervals than designed for. Hence, freezing of the grout becomes more likely.

Freezing and thawing lead to changes in state of stress and consequently may lead to changes in soil or grout structure. Due to occasional events of damage caused by frozen BHEs, authorities in central Europe became aware of this potential hazard (Bassetti et al. 2006). As a consequence, several authorities do not permit working fluid temperatures below 0.0°C, or prescribe the usage of water as working fluid; others claim that grouting materials used for BHEs have to be frost-resistant. If peak working fluid temperatures below 0.0°C are prohibited, the length of the BHEs must be increased in order to cover the peak heating demand, resulting in higher drilling and material costs.

Freezing and thawing stresses on soils, concrete, paper sludge, and bentonite fillings have been evaluated widely (e.g., Konrad and Morgenstern 1980; Moo-Young and Zimmie 1996). There is a wide variety of directives and standards for testing procedures and required material properties (e.g., ASTM D-6035-08). Unfortunately none exists specifically for BHE grout materials.

Due to broad experiences in cyclic freeze-thaw-tests for concrete and natural stones, most previous grout tests were based on existing procedures. These focus on the assessment of mechanical properties like compressive strength or the loss of weight caused by frost. As a consequence, many grouting materials in Europe were modified in order to pass concrete-frost-tests. However, the mechanical properties do not necessarily correlate with the hydraulic properties which are mandatory for the groundwater protection. Existing standards for freeze-thaw-testing of grout are not applicable due to the specific thermal, hydraulic, and mechanical boundary conditions of BHEs.

The presented experimental procedure assesses the susceptibility of grouting materials to cyclic freeze thaw stresses. As the focus of this procedure is on the sealing properties of the material, the hydraulic conductivity is measured as the crucial parameter. The theoretical background of the in situ freezing process will be discussed. The construction of the testing device and its setup will be outlined. A numerical and experimental verification of the temperature distribution inside the testing device will be supplied. The experimental results of tested grouts will be presented and discussed.

#### TESTING GROUT FOR BHEs

As grouting materials have to meet a broad range of requirements such as sealing, resistance against erosion of the backfill, suitability for pumping, sufficient thermal conductivity, etc., special materials were developed (e.g., Allan and Philippacopoulos 1998).

The backfill seals the borehole if aquicludes are penetrated. Thus, unwanted hydraulic connections between aquifers are prevented. Furthermore, it provides a protection layer that prevents any leakage of the working fluid to the groundwater. On the other hand, it has to provide a sufficient heat flux towards the BHE (VDI 2001; Mehnert 2004). From a hydrogeological point of view, the thermal requirement is of secondary priority; the proper sealing of eventual penetrated aquicludes is of prime importance. This hydraulic sealing of penetrated aquicludes is the critical property that is tested by the developed device.

The testing device measures the hydraulic conductivity. The presented hydraulic conductivity is calculated according to the European standard (CEN ISO/TS 17892-11 2004):

$$(1) \quad K = \frac{\Delta V \times L \times \alpha}{A \times \Delta h \times \Delta t}$$

where:

$K$  = hydraulic conductivity, calculated at 10.0°C (50.0°F)  
groundwater temperature,

$V$  = volume of water collected in time,  $\Delta t$ ,

$\Delta L$  = length of the specimen,

$\alpha$  = correction factor for testing fluid viscosity,

$A$  = cross sectional area of the specimen,

$\Delta h$  = change in water head along the flow path  $\Delta L$  and

$\Delta t$  = time.

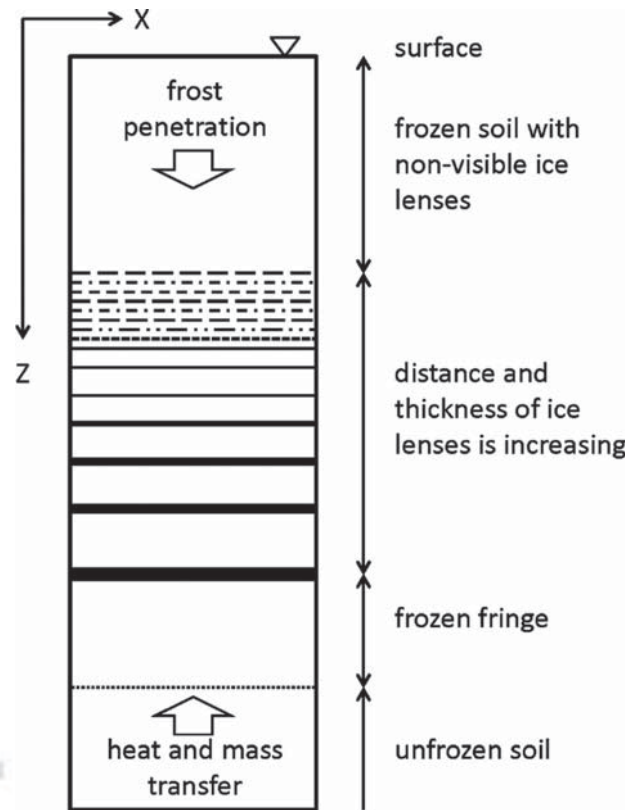
### Direction of Freezing

The direction of freezing controls the location and orientation of ice lenses and thus the subsequent damage to the material. Frost heaving processes and ice lens growth in fine grained soils have been widely analyzed (Konrad and Morgenstern 1980; Ono 2002; Coussy 2005; Unold 2006). The influence of frost on hydraulic conductivity has been quantified for paper sludge and bentonites in several investigations and an ASTM Standard was established in 2008 (ASTM D6035-08). The ASTM D6035 Standard requires either a one-dimensional or a three-dimensional freezing process.

Following the one-dimensional approach, cylindrical specimens are insulated radially, so the frost penetrates vertically. This leads to an ice lens growth perpendicular to the  $z$ -axis (Ono 2002; Unold 2006; Bronfenbrener and Bronfenbrener 2010). In fact, horizontal ice layers grow, just like the in situ freezing process of fine grained soils (Fig. 1). Thus the mechanism reflects many in situ freezing situations. A subsequent hydraulic conductivity test in the vertical direction simulates water penetration. The direction of water flow is perpendicular to the ice-induced disruptions. For the assessment of the hydraulic sealing of BHEs the one-dimensional approach does not reflect the in situ boundary conditions.

The 3D freezing is often used for testing the frost-resistance of soils, concrete, or natural stones. Executing these

**FIG. 1** Schematic illustration of rhythmic ice lens formation in fine-grained soils (Konrad and Morgenstern 1980; Unold 2006).



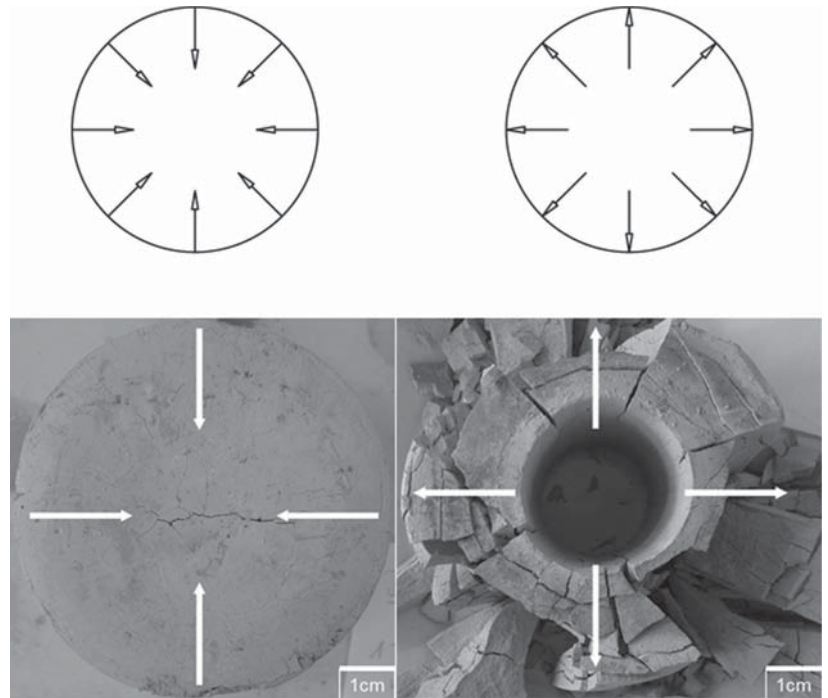
tests, specimens are frozen without any insulation to allow the heat flow to exit the specimen's surface in all directions. This leads to a spherical ice lens growth. The structural disruptions do not reflect the crack patterns of frozen BHEs. Thus 3D freezing is not appropriate for the assessment of grout material for BHEs.

For BHEs the frost penetrates radially in a two-dimensional way (Carslaw and Jaeger 1959; Philippacopoulos and Berndt 2001; Sass and Lehr 2011). As ice lenses grow perpendicular to this direction, they are of a cylindrical shape. These disruptions have the same orientation like the critical fluid flow path of a BHE. Hence the application of the 1D and 3D approaches do not reflect the in situ freezing mechanism and cannot lead to valid statements about the freeze-thaw influence on hydraulic conductivity.

The specimens must be frozen two-dimensional and in the radial fashion (Fig. 2). Comparing the left and the right images of Fig. 2 it is evident, that the differences in freezing directions lead to different states of stress, shown by the cracking pattern. Considering the in situ process of a freeze-thaw-cycle in a BHE, it is of great importance to follow the freezing direction from inside out.

**FIG. 2**

Influence of the freezing direction on the location of ice lenses/ material disruptions; left: grout specimen frozen 3D from outside in, no expansion constraints, unlimited water supply (bottom side); right: grout specimen frozen 2D from inside out, all side expansion constraints and unlimited water supply. Both specimens were prepared under the exact same conditions, stressed by 1 FTC (20 h,  $-10.0^{\circ}\text{C}$ ) and subsequently dried.



In the area where pore water first freezes in a soil, it is very likely that phase change from liquid water to frozen water occurs without visible ice lens growth as outlined in **Fig. 1** (Konrad and Morgenstern 1980; Unold 2006).

For a given overburden pressure, ice lens growth is a function of water supply and the gradient of heat loss. Near the surface of fine grained soils or grouting materials, there is not enough water for the accumulation of ice lenses. This is caused by the relative low hydraulic conductivity of these materials. A suction process begins from the inner structure towards the freezing-front. With increasing distance from the point of frost penetration, the probability of ice lenses increases as water supply becomes sufficient. When taking a closer look at the described testing procedure, not only the axis of frost penetration is important, but also the direction (**Fig. 1**). A grout specimen frozen from outside in receives its crucial disruptions in the centre (**Fig. 2**, left). A specimen frozen vice versa, from inside out, has its heaviest disruptions at the outer edge (**Fig. 2**, right). This is because ice lenses grow in the direction of heat loss.

Comparing the crack patterns of the specimens shown in **Fig. 2** with the schematic process of ice lens growth in fine grained soils (**Fig. 1**), it is evident that these mechanisms correlate. The ice lens thickness increases with increasing distance from the coldest surface in contact with the soil. When the soil thaws, cracks result from the ice lens formation. This mechanism corresponds to the radial mechanism in the testing device.

Thus a testing procedure that assesses the change in material structure due to freezing-processes has to follow the in situ freezing directions. In the case of BHEs: radially from inside out.

### Boundary Conditions

During the freezing process, ice lens growth often occurs, inducing volumetric change. In situ earth pressure partially hinders the volumetric expansion (ASTM D-6035-08). Therefore a testing procedure should have a confining radial cell-pressure that reflects the geomechanical boundary conditions in a BHE.

## Materials and Methods

### TESTING DEVICE

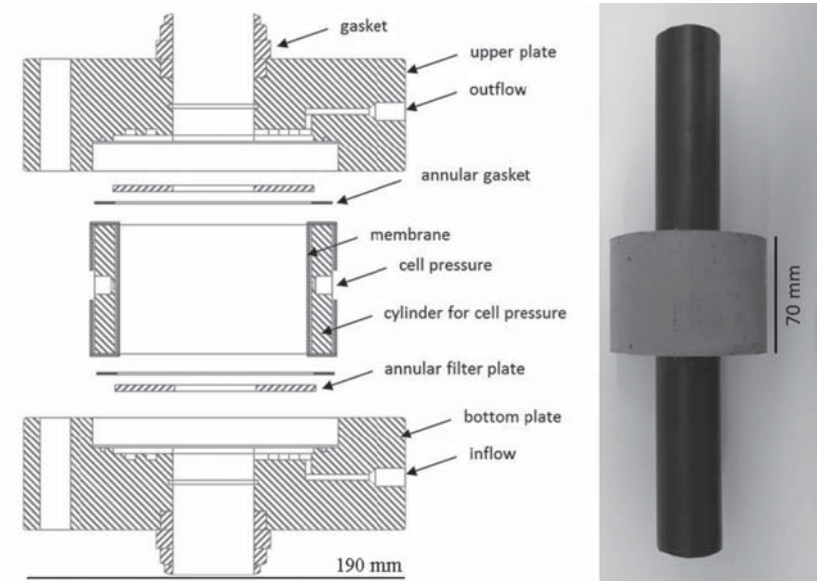
The testing device is a modification of a triaxial flexible wall permeameter (**Fig. 3**). Specimens are fixed between an upper and a lower filter plate. These filter plates provide a uniform water flow for water permeability testing and prohibit axial expansion induced by phase change and ice lens growth. Water pressure can be applied via the filter plates and connections to the laboratory equipment.

Cell pressure is applied between a membrane and a cylindrical rigid ring as abutment. Thus unplanned tangential water flow between the membrane and the lateral surface of the specimen is prevented. Furthermore, a radial pressure can



Ansichtsexemplar. Keine Vervielfältigung erlaubt.

**FIG. 3**  
Schematic of the testing device (left) and specimen for freeze-thaw-testing (right).



be applied, simulating earth pressure. The fluid for the cell pressure is not in contact with the specimen itself. As the cell pressure must not vary during the freezing tests, the fluid is a mixture of water and glycol which provides sufficient frost protection and thus remains in a liquid state at temperatures below 0.0°C.

Due to the special shape of the specimens, gaskets are fitted in the upper and bottom plate. The gaskets seal the device and prevent unwanted loss of the testing fluid. As the grouting material has to seal the BHE primarily in a vertical direction, the testing device measures the hydraulic conductivity along the axis of the specimen. The testing device has a diameter of 19.0 cm and a total height of 46.0 cm inclusive stand and connections to the recirculation thermostat. With its relative small dimensions, the device can be implemented in any laboratory that possesses an apparatus for the determination of hydraulic conductivities of soils.

**SPECIMENS**

As the specimens represent a vertical slice of a BHE, they are composed of a length of a pipe (simulating the probe) and the grout itself (Fig. 3, right). For consistent and standardized testing with comparable results, specimens have to be of exactly identical shape. In this case, a perfectly axial embedment of the pipe into the surrounding grout body is obtained.

The design is analogous to the one chosen by Sugama (2006) in order to assess the shear-bond-strength of grout and steel pipes. By choosing high density polyethylene (HDPE)-Pipes instead of steel the specimens simulate the system of a BHE. Furthermore the ratio of cross-sectional area ( $A_{Grout}$ ) to circumference of the probe ( $C_{Probe}$ ) embedded in the specimen was calculated true to scale (see Fig. 4 and Eq 2). Figure 4 shows the horizontal cross-section of a BHE with its probes and the grout body (left) and the cross-section of the designed specimen (right).

**FIG. 4**  
Schematic of the specimen design. Left: BHE with a closed double-U-loop; Right: Specimen for freeze-thaw-testing.

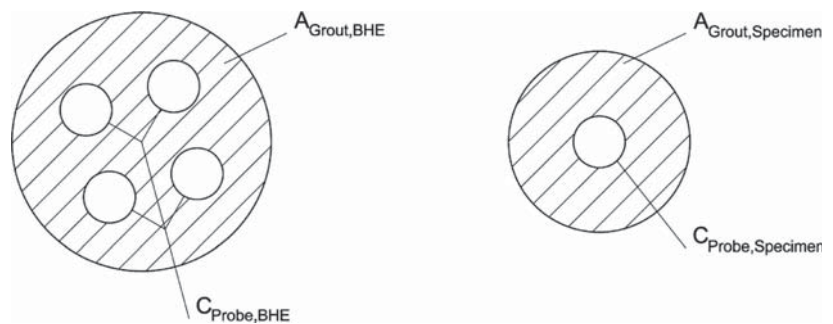


**TABLE 1** Dimensions for specimen design.

Parameter	Specimen	BHE
Diameter grout	96 mm	150–180 mm
Diameter probe	40 mm	4 × 32 mm
Length grout body	70 mm	–
Length of probe	350 mm	–

As the most common design of BHEs in Europe is the double-U-loop-type, the calculation was based on it. Assumptions for the calculation are shown in **Table 1**. As the geometrical relations (Eq 2) of the BHE and the specimen are comparable, the relative increase in hydraulic conductivity due to imperfect bonding between grout and pipe is considered to match in situ conditions.

$$(2) \quad \frac{A_{\text{Grout,BHE}}}{C_{\text{Probe,BHE}}} = \frac{A_{\text{Grout,Specimen}}}{C_{\text{Probe,Specimen}}}$$

The specimens have an axial-symmetrical geometry; the actual position of the probe in situ will most likely vary from this idealized design. It is obvious that the chosen specimen design will lead to a higher hydraulic conductivity than specimens of bulk grout. The contact area of the hydrophilic grout and hydrophobic HDPE is a preferred water path (Allan and Philipacopoulos 1998; Baumann et al. 2003). As the water can flow along the surface of the pipe and through the grout, the tested vertical hydraulic conductivity will be higher than the conductivity of bulk grout. In a BHE, another area of increased fluid velocity is the surface between the grout and the surrounding soil. However, the connection of these two hydrophilic materials (grout and soil) is only of little importance to the systems' sealing (Baumann et al. 2003). Consequently, the most critical flow path is tested.

Due to a significant dependence of the grouting material properties on the effective temperature during the hydration process, the storage of the specimens has to follow in situ temperature levels. The specimens have to be stored in a

temperature-controlled chamber. In this case, the temperature of the chamber was set to 8°C (46.4°F).

As the grout needs to prevent the BHE from hydraulic connection with the penetrated aquifer, the most critical section of the BHE is where an aquiclude is sealed. Aquicludes are not necessarily fully saturated and water supply is not necessarily unlimited. This has to be considered for specimen preparation. In this case, no water curing was executed, but evaporation was prevented. The water content of the mixed grout needs to suffice for cement hydration. Consequently, the most critical in situ case is simulated.

Casting systems were constructed as presented in **Fig. 5** for a standardized specimen preparation.

The casting system fixes the pipe in the axial middle of a cylinder. The cylinder is lubricated with petroleum jelly in order to minimize bonding between grout body and casting system. The casting cylinder can be opened from the side (**Fig. 5**, right). Thus specimens can be easily removed. The cylinder is bordered by an upper and a bottom plate.

After removing the specimen from the casting system, the grout body of the specimen is trimmed in axial length to a cylindrical shape (**Fig. 3**, right). The axial surface of the grout body has to be perfectly even.

#### TESTING SETUP

After a defined setting time (in this case, 28 days of curing) the grout specimen is transferred into the testing device. The testing device is closed up, gaskets are tightened, and the pipes and the device are filled with de-ionised water (ASTM D-5084-10). The upper and lower cross-sectional area of the grout is enclosed tightly by the filter plates of the testing device during testing. The specimens are saturated and the saturation is controlled (CEN ISO/TS 17892-11:2004, 2005). For saturation, the back pressure is applied stepwise to a level of 200.0 kN/m<sup>2</sup> (29.10 psi) and a cell pressure of 250.0 kN/m<sup>2</sup> (36.26 psi). By setting the pressure drop to a delta of 21.0 kN/m<sup>2</sup> (3.05 psi) water flow is applied. According to ASTM D-5084-10, the pressure of the headwater is increased in order to prevent any solving of air

**FIG. 5**

Casting systems. Left: Closed casting systems; Right: casting cylinder (opened to the side).

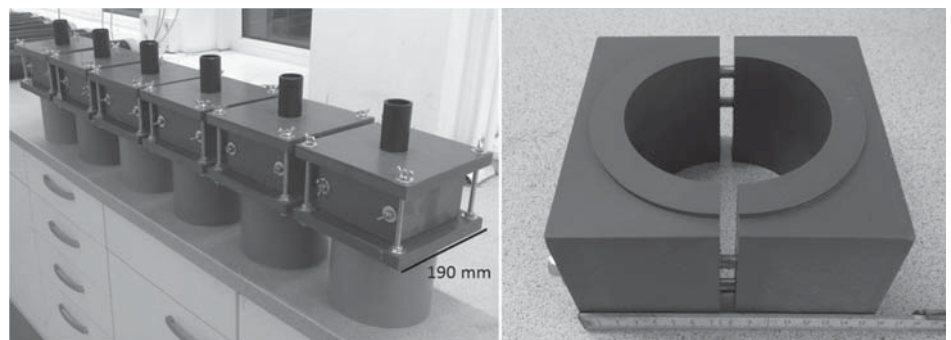
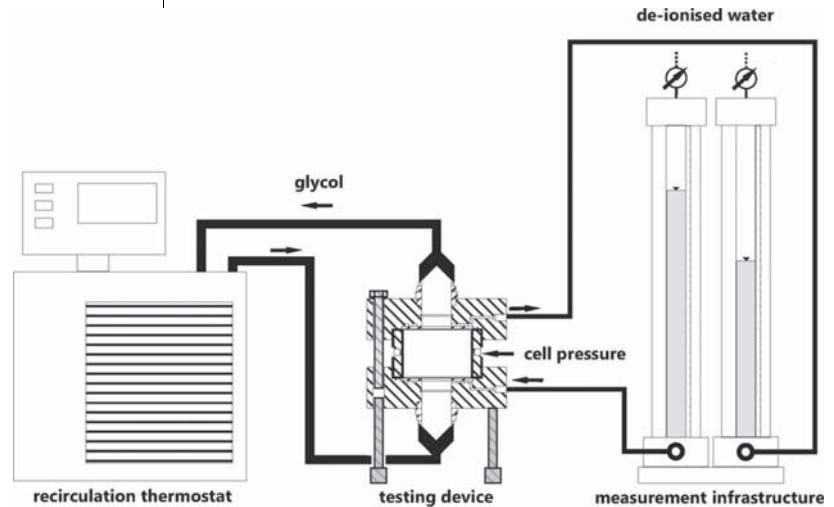


FIG. 6

Schematic of the testing setup.



Ansichtsexemplar. Keine Vervielfältigung erlaubt.

bubbles from the backpressured specimen water caused by falling water pressure. Saturation is controlled by documentation of the change in hydraulic conductivity and the difference between inflow and outflow. Thus it is feasible to check if the saturation is completed. The determination of the hydraulic conductivity is commenced when full saturation is given.

For freeze-thaw-simulation saturation pressure is applied again in order to provide an unlimited water supply during the freezing process (Ono 2002; Unold 2006). The temperatures causing freezing and thawing are provided by a circular flow of working fluid through the pipe of the specimen. Working fluid temperature is controlled by a heat pump (Fig. 6). Specimens are allowed to freeze completely and then thaw again.

Any number of freeze-thaw-cycles and measurements of hydraulic conductivity may be executed with the testing device. A recirculation thermostat pumps a working fluid through the pipe of the specimen. Ground source heat pump systems in regions with long heating periods often run with working fluid temperatures of  $-4.0^{\circ}\text{C}$  ( $24.8^{\circ}\text{F}$ ) down to  $-7.0^{\circ}\text{C}$  ( $19.4^{\circ}\text{F}$ ) according to the directive VDI 4640 (2001). Freeze-thaw-testing procedures for other construction materials like concrete, gravel, or geosynthetic clay barriers use temperatures between  $-5.0^{\circ}\text{C}$  ( $23.0^{\circ}\text{F}$ ) (CEN-TS 14418:2005, 2006) and  $-20.0^{\circ}\text{C}$  ( $-4.0^{\circ}\text{F}$ ) (EN 1367-1:2007). According to ASTM D-6035, most damage in the hydraulic conductivity occurs with freezing temperatures between  $0.0^{\circ}\text{C}$  ( $32.0^{\circ}\text{F}$ ) and  $-15.0^{\circ}\text{C}$  ( $5.0^{\circ}\text{F}$ ). For freezing simulation the thermostat cools the fluid to a temperature level of  $-10.0^{\circ}\text{C}$  ( $14.0^{\circ}\text{F}$ ) within 2 h. The cooling velocity is based on typical heat pump working cycles (Anbergen et al. 2013). Thus the specimen freezes from inside out. In order to prevent superfreezing (ASTM D-6035-08), a lower temperature level was not chosen. An insulation surrounding the testing device was applied to reduce heat flow

towards specimens. Using a Finite Element Analysis, the required freezing times are calculated and controlled by a temperature log. The time for freezing is set to a value of 20 h, so is thawing time. For thawing, the temperature of the working fluid is set to  $+8.0^{\circ}\text{C}$  ( $46.4^{\circ}\text{F}$ ) in order to provide a moderate thawing. The thawing temperature equates to the curing temperature during specimen preparation. After each FTC, the hydraulic conductivity is measured. Thus, the potential change in hydraulic conductivity in a field installation can be quantified.

The following diagram (Fig. 7) shows the characteristic temperature curves of the freezing process of three testing devices at the same time.

The temperature was logged between the outer edge of the cylindrical grout specimen and insulation every 300 s. It is noticeable that the phase change from water to ice influences the measured temperature. The latent heat influence can be observed during freezing and thawing temperature log.

Performing one freeze-thaw-cycle including the subsequent determination of hydraulic conductivity takes 48 h.

## Results

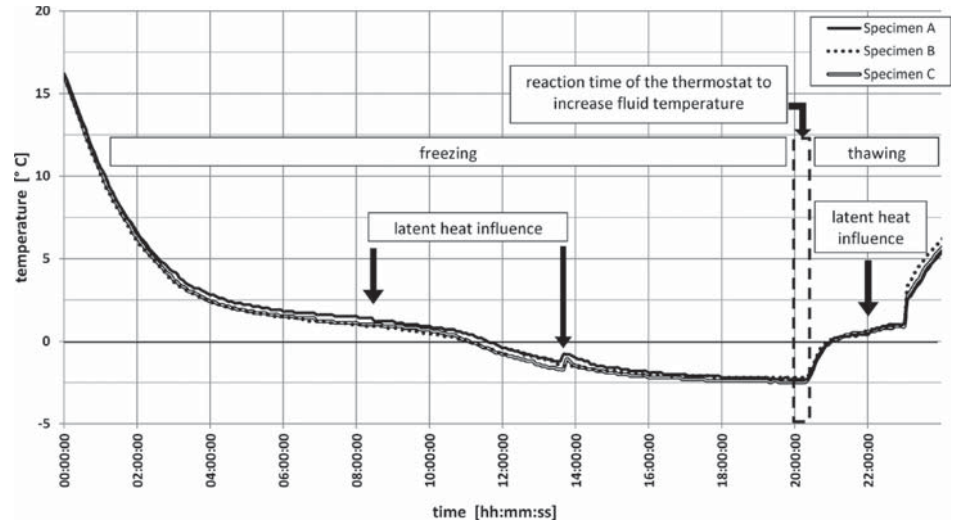
### HYDRAULIC CONDUCTIVITY TEST

The testing results of three different common grouting materials for BHEs are presented. The grouts used are commonly used in the geothermal drilling industry. Solid substances only need to be mixed with water and do not require any additives. The suspensions were prepared using a paddle mixer with 300 rpm. After 5 min of mixing, the suspensions were filled into a new container and mixed for two additional minutes. Three specimens of each material were tested in order to verify the reproducibility of the results. The specimens were prepared under the exact same conditions. For each grout material the ratio of



FIG. 7

Temperature log of one freeze-thaw-cycle.



water to solid substance (W/SS) and the density of the suspension are presented in **Table 2**. As the grouts are industrial mixtures, the exact compositions of the grouts are not a matter to be published. However, the Grouts A and B are thermally enhanced in order to provide an enhanced heat transfer. Furthermore, only grout B contains clay minerals which are likely to swell.

The hydraulic conductivities are measured before and after cyclic freeze-thaw-stress. The results of these tests are shown in **Fig. 8**.

The increase in hydraulic conductivity with increasing number of cyclic freeze-thaw-stresses is evident. This increase depends on the grouting material's properties. The hydraulic conductivities of the three tested grouts are in the order of magnitude at  $1 \times 10^{-07}$  m/s. These results resemble prior grout/probe tests of neat cement mixtures (Allan 2000). Certain grouts have a low susceptibility to cyclic freeze-thaw-stresses (Grout B) and other materials are strongly influenced by the testing procedure (Grout C).

The first freeze-thaw-stresses have a higher influence on the permeability than the following ones. These findings correspond with the ASTM D-6035-08 and the investigations of Moo-Young and Zimmie (1996).

When evaluating these results, it is worth noting that the influence of the frost on the hydraulic conductivity declines with increasing number of FTCs. The first FTC induces the

greatest increase in hydraulic conductivity. As there is a trend of a decreasing influence of the FTCs, it is possible to make a statement on the frost resistance of grouting materials within a reasonable number of thermal stresses.

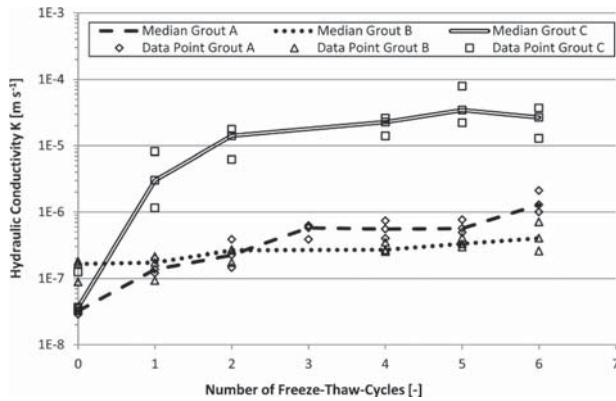
There is a significant difference in hydraulic conductivity when testing the raw grout material or the system grout/probe. These results have been confirmed by prior investigations (Allan and Philippopoulos 1998; Allan 2000). The surface between grout body and probe is a preferred flow path. In this survey, it was quantified that the difference in hydraulic conductivity is of around two orders of magnitude. **Figure 9** shows three hydraulic conductivities of each material: first the conductivity of the raw grout, second the conductivity of the system grout and probe before any freezing stress. The third symbol marks the K-value of the system grout and probe after six cyclic freeze-thaw-stresses.

The specimens of the raw grout were prepared under the exact same conditions as the grout/probe specimens. The specimens were of a cylindrical shape of 70 mm length and had a diameter of 96 mm. The same water/solid substance-ratio was used as described in **Table 2**. Again, specimens did not cure underwater, but with prevention of evaporation. The setting time was 28 days at 8.0°C before commencement of saturation and subsequent testing. The hydraulic conductivity was tested according to CEN ISO/TS 17892-11:2004 in a flexible wall permeameter. The hydraulic conductivities of the bulk materials

**TABLE 2** Relevant characteristics of the three tested grouting materials.

Grout Type	Ratio W/SS	Suspension Density	Thermally Enhanced	Contains Swelling Clay Minerals
Grout A	0.55	1.66 g/cm <sup>3</sup>	+	-
Grout B	0.60	1.64 g/cm <sup>3</sup>	+	+
Grout C	0.70	1.62 g/cm <sup>3</sup>	-	-

**FIG. 8** Hydraulic conductivity of specimens of three different grouting materials in dependence on the number of freeze-thaw-cycles.



are of an order of  $1 \times 10^{-10}$  m/s. Prior investigations on cement pastes and grouts resulted in lower hydraulic conductivities (Allan and Philippopoulos 1998). This is because the setting conditions were substantially different. In this study, in situ conditions are simulated first. The decreased temperature and the limited water supply result in changed material properties as the hydration process itself is influenced.

**FROST INDUCED CHANGE IN STRUCTURE**

During the phase change of water and ice lens growth volumetric change occurs. This change exerts pressure that stresses the solid structure of the grout. It can be observed that the hypothesis of a radial heat flow and thus an axis-parallel frost front is confirmed. Frost induced disruptions in the specimens (Fig. 10)

**FIG. 9** Hydraulic conductivity of specimens of three different grouting materials. Comparison of the sole materials' hydraulic conductivity and systems' hydraulic conductivity before and after freeze-thaw-stresses.

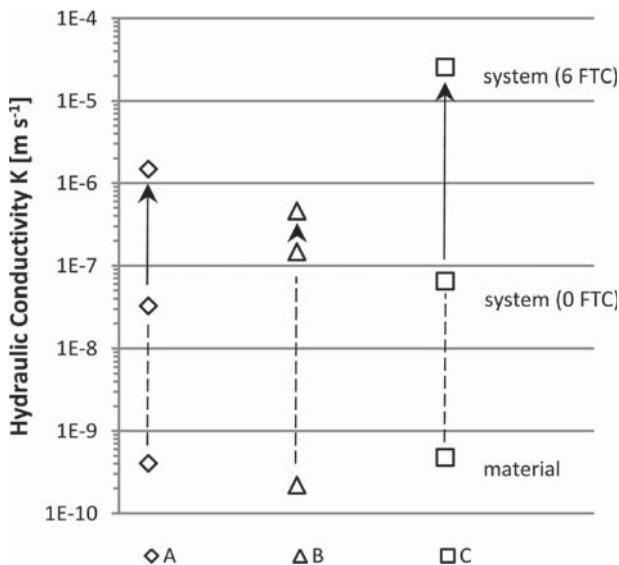
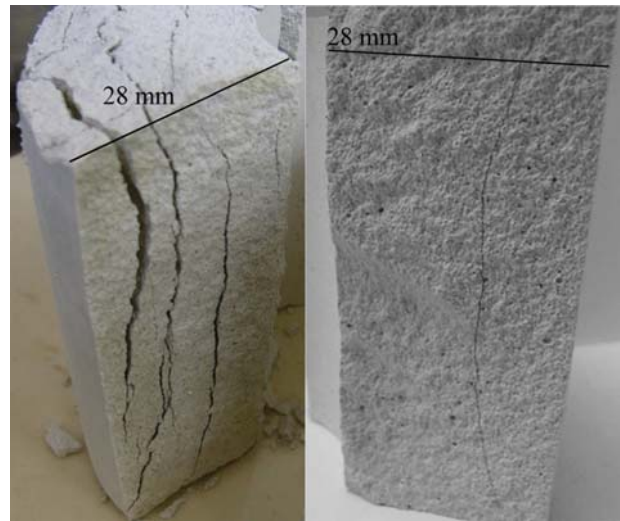


**FIG. 10** Frost induced cracks in specimens of grout A (left) and grout C (right) after six freeze-thaw-cycles and subsequent drying.



are mostly parallel and in the axial direction. Cracking occurs in a cylindrical pattern. Specimens shown in Fig. 10 were subjected to six freeze-thaw-cycles. Grout A (left) and grout C (right) both show vertical cracks. The materials are marketed as resistant to cyclic freezing stresses and are frequently used for BHEs. After testing, specimens were thoroughly dried at 105.0°C (221.0°F) removing all water from the specimen to prevent any effects of apparent cohesion.

These cracks are preferred paths for water flux; however, not every crack will inevitably increase the hydraulic conductivity of the specimen. Whether a crack has a great influence on the sealing effect or not, primarily depends on the content of swelling clays, e.g., bentonite. If a disruption occurs it is very likely that fine-grained components will swell, reduce the width of the crack and reduce water flux. There are certain grouting materials that are not prone to cyclic freeze-thaw-stresses. Figure 11 shows a specimen of a grout B without visible frost induced disruptions after six freeze-thaw-cycles.

**FIG. 11** Specimen of grout B after six freeze-thaw-cycles and subsequent drying.

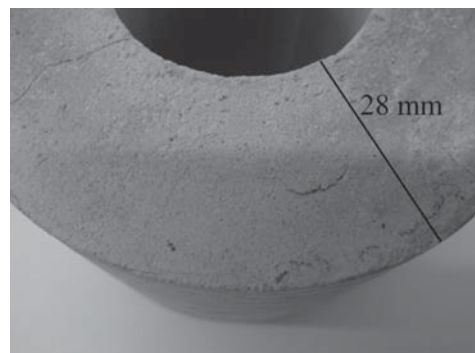
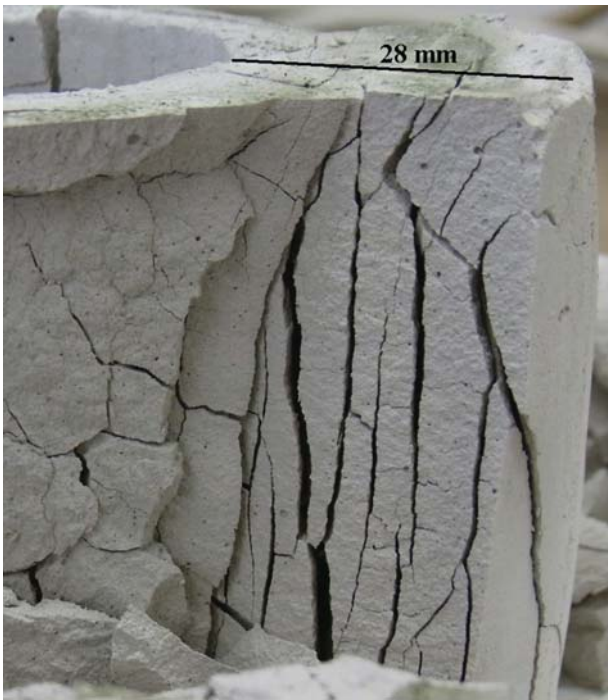


**FIG. 12** Frost induced cracks in specimen after one freeze-thaw-cycle and subsequent drying.



The specimens of grout B display the lowest hydraulic conductivity after six freeze-thaw-cycles. This correlates with the visual observations of the cracking patterns.

In order to verify the influence of the swelling clay content on the freeze-thaw-resistance and the cracking pattern, another grouting material was tested. This grout is not thermally enhanced and contains no swelling clays. Again, the setting conditions were exactly the same. The specimens were subjected to one freeze-thaw-cycle and subsequently dried (Fig. 12).

The disruptions are vertical. It is obvious that the cracks appear perpendicular to the propagation of the frost front. These are typical frost induced disruptions and correlate with the disruptions of the other tested grouts. The grout without swelling clays is highly influenced by the FTC.

During the thawing process, the frost induced vertical cracks formed (Fig. 12). The cracks of this specimen underpin the need of a confining radial pressure. Specimens tested without such a restriction, could expand laterally and cracks gape open during the testing procedure.

#### VERIFICATION OF THE TEMPERATURE DISTRIBUTION INSIDE THE TESTING DEVICE

As the testing procedure aims to simulate the in situ freezing directions, two verifications are outlined in this paper. On the one hand, a numerical model of the temperature distribution is presented; on the other hand, an experimental approach with surface temperature measurement is made.

**TABLE 3** Thermal properties of the solid components of the modeled testing device (see Fig. 3 and Fig. 13, left).

Component	$\varepsilon^a$ (-)	$\lambda^b$ ( $\text{Wm}^{-1}\text{K}^{-1}$ )	$c^c$ ( $\text{MJK}^{-1}\text{m}^{-3}$ )
Probe	$1 \times 10^{-6}$	0.40	1.900
Grout	0.6	2.00	4.560
Filter plate	0.54	60.00	3.318
Upper and lower plate	$1 \times 10^{-6}$	0.17	2.100
Membrane	$1 \times 10^{-6}$	0.16	1.587
Insulation	$1 \times 10^{-6}$	0.04	0.066

<sup>a</sup> $\varepsilon$  = porosity.

<sup>b</sup> $\lambda$  = thermal conductivity of solid.

<sup>c</sup> $c$  = volumetric heat.

#### NUMERICAL MODEL

The thermal process is modeled with the finite element modeling code FEFLOW. Since there are components of the testing device which are highly porous (filter plates and grout material) thermal hydraulic coupling is applied. Thus the hydraulic influence on the thermal distribution inside the modeled testing device is respected. The coupled conductive and convective heat-transport is calculated according Eq 3.

$$(3) \quad (\rho c)_g \frac{\partial T}{\partial t} = \nabla \cdot (\lambda \nabla T - \rho_f c_f \mathbf{q} T)$$

where:

$(\rho c)_g$  = bulk volumetric heat ( $\text{J K}^{-1} \text{m}^{-3}$ ),

$T$  = temperature ( $^{\circ}\text{C}$ ),

$\lambda$  = thermal conductivity tensor ( $\text{W K}^{-1} \text{m}^{-1}$ ),

$\rho_f$  = density of fluid ( $\text{g m}^{-3}$ )

$c_f$  = heat capacity of fluid ( $\text{J g}^{-1} \text{K}^{-1}$ )

$\mathbf{q}$  = Darcy velocity ( $\text{m s}^{-1}$ ) (Rühaak and Sass 2013)

An excerpt of the assumed material properties is shown in

#### Table 3.

As the testing device is axisymmetric, the numerical model can be simplified (Fig. 13, left). The 2D sketch of the device is calculated as a rotationally symmetric body (compare to Fig. 3, left).

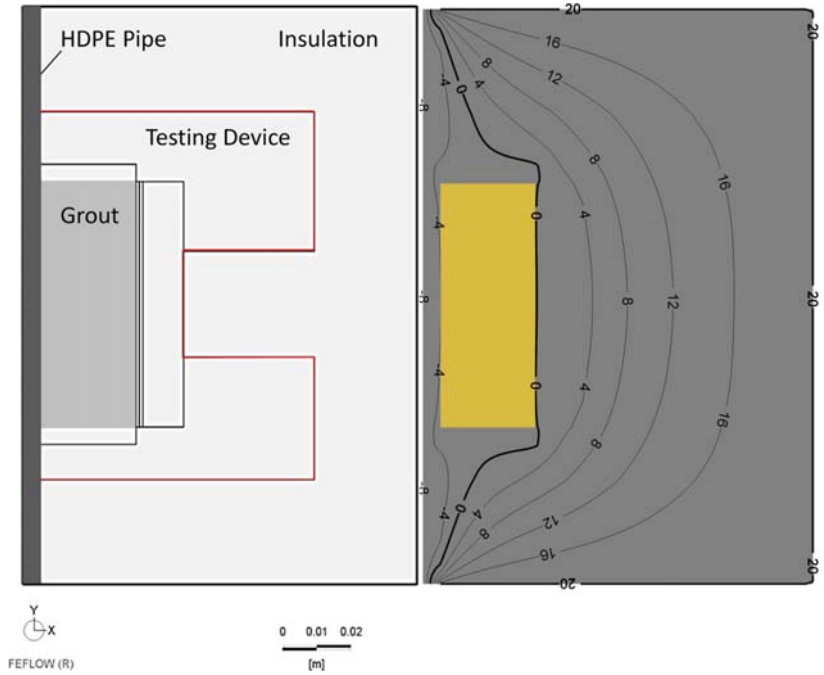
The left-hand edge of the model represents the inner wall of the pipe. It is assumed that the temperature profile of the working fluid streaming through the pipe is constant along the axis. Thus a constant temperature boundary condition is set during the freezing and thawing process.

The described numerical model allows predictions of the temperature distribution within the grout body of the specimens. The right-hand side of Fig. 13 shows the calculated temperature distributions after 15 h of freezing. The isothermal lines are given in degrees Celsius. With increasing time the frost front ( $0.0^{\circ}\text{C}$ -line) propagates radially. The isothermal lines inside the specimen are of a foremost vertical shape. Thus the numerical solution confirms the assumption that temperature propagation inside the specimen corresponds to the in situ process in a grouted BHE.



**FIG. 13**

FEFLOW model of the testing device (left) and calculated temperature distribution (isothermal lines) after 15 hs of freezing (right). Grout specimen—highlighted; temperatures in °C.



**THERMAL IMAGING**

As an experimental verification of the temperature distribution, thermal imaging was applied to the frozen specimens. Therefore specimens are prepared and subjected to the described testing procedure. After defined time intervals (here: 4, 5, and 15 h) freezing is stopped, the testing device is opened, specimens are cut open and a thermal image is taken (Fig. 14). Thus temperature distribution on the split-area of the grout body is recorded and the propagation of the frost front can be observed. For each time interval a separate specimen is used.

The presented thermal images (Fig. 14) are those of three selected time intervals. Due to the splitting process there are disturbances at the outer edge of the specimen (right-hand edge of Fig. 14(a)). Since the surface temperatures are measured, these disturbances have an influence on the results and need to be considered for the evaluation. The inner structure of the specimens is not thermally affected by the splitting process and

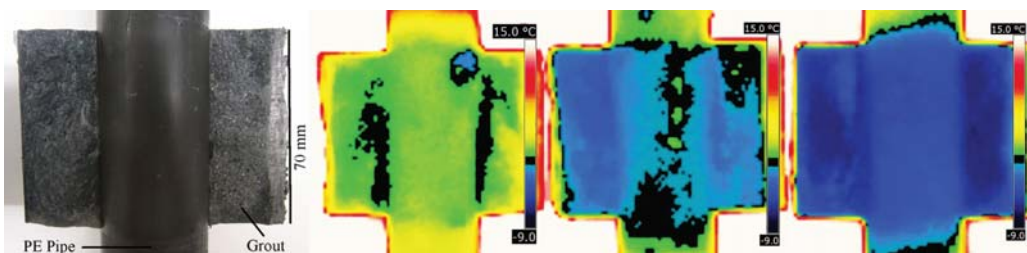
consequently the thermal distribution inside the specimen can be quantified.

After 4 h of freezing (working fluid temperature of  $-10.0^{\circ}\text{C}/+14.0^{\circ}\text{F}$ ), the temperature of the grout body has decreased. Temperature at the inner edge of the grout body is lower than the temperature at the outer edge (Fig. 14(b)). In the near field of the probe, the temperature has dropped below  $0.0^{\circ}\text{C}$ . The temperature scale is shown in the graphic and ranges from  $+15.0^{\circ}\text{C}$  ( $59.0^{\circ}\text{F}$ ) to  $-9.0^{\circ}\text{C}$  ( $15.8^{\circ}\text{F}$ ). The range of  $0.0^{\circ}\text{C}$  ( $32.0^{\circ}\text{F}$ ) to  $-1.0^{\circ}\text{C}$  ( $30.2^{\circ}\text{F}$ ) is marked separately on the scale (black).

Temperature inside the grout body decreases with increasing time of freezing. The propagation of the frost front (respectively, the isothermal line of  $0.0^{\circ}\text{C}$  where freezing can occur) has a foremost vertical shape and moves radially from the inside to the outside.

With further increasing time temperature continues to decrease. After 5 h, the temperature of nearly the whole

**FIG. 14** Photograph of a specimen (split up) prepared for thermal imaging (a) and thermal images of specimens after 4 (b), 5 (c), and 15 (d) hours of freezing.





specimen has dropped below  $0.0^{\circ}\text{C}$  (Fig. 14(c)). During the following freezing time, temperature of the whole specimen drops below  $0.0^{\circ}\text{C}$  (Fig. 14(d)) and remains in freezing temperature conditions until thawing is initialized.

The thermal imaging shows that the freezing process inside the specimens corresponds to the radial shape of the freezing in BHEs and the numerical results. Since temperature is below  $0.0^{\circ}\text{C}$ , ice lens growth is possible.

## Discussion

The hydraulic conductivity of BHEs primarily depends on two preferred paths for water flux; the contact surface between grout and probe and the contact surface between grout and surrounding soil. The presented testing device takes only the first mentioned pathway into account. As this testing procedure aims to assess the freeze-thaw-resistance of the grouting material in a standardized way, the interaction between grout and soil has to be excluded. Furthermore, the path along the surface of the probe is the more critical hydraulic connection due to the hydrophobic properties of probe. This hydraulic connection apparently leads to a higher hydraulic conductivity of a magnitude around two (Fig. 9) compared to the bulk hydraulic conductivity. These results have been confirmed by prior investigations on back-fill grout materials (Allan and Philippacopoulos 1998). The hydraulic conductivity tests were executed at laboratory temperature level of about  $20.0^{\circ}\text{C}$ . Due to different thermal expansion coefficients of grout and probe, there will be a dependence on the temperatures during determination on hydraulic conductivity (Allan 2000). As the specimens cured under in situ temperature conditions and were tested at laboratory temperature level, this influence will be relatively small.

On the other hand, the influence of the curing temperature on the hydraulic properties of the grouts is evident. The hydration process of the cement components is strongly temperature dependent. This has to be taken into account for a proper characterization of grouting materials. Particularly when groundwater protection issues are discussed and minimum requirements on material properties are set, the in situ conditions need to be considered. In some cases, grout testing for water-saturated subsurface conditions could be done with setting conditions with unlimited water supply. Furthermore, if the groundwater temperature varies substantially as opposed to the assumptions made here, the setting temperature has to be changed.

The results of the numerical modeling correlate very well with the experimental observations. The propagation of the frost front is foremost perpendicular to the axis of the specimen. The frost front moves radially from the inside to the outside.

## Conclusion

The developed testing procedure produces feasible and reproducible results that represent thermal and hydraulic conditions of BHEs in the field. The hydraulic conductivity of the three tested materials increases with cyclic freeze-thaw-stresses. Frost induced cracks occur vertically in the direction of the most critical hydraulic pathway. With the presented procedure, a standardized assessment of grouting materials for BHEs under freeze-thaw-stresses can be supplied. The increase depends on the type of grouting material. Grout B shows the least increase in hydraulic conductivity and no visible frost induced cracks. This grouting material is the only one that contains swelling clay minerals. The tested grouts without swelling clay components are more susceptible to cyclic freeze-thaw-stresses.

## Outlook

The testing device can be implemented easily in any geotechnical laboratory that possesses an apparatus for hydraulic conductivity testing. With its handling and high precision, the procedure can contribute to quality assurance for shallow geothermal systems. Specimens can be prepared easily and freeze-thaw-tests can be executed at reasonable expenses. As the casting system is very flexible, it can be used for a quality control of grouting materials on site. These specimens can be tested after a defined setting time and the results of the freeze-thaw-test could decide whether the BHE may run with fluid temperatures below  $0.0^{\circ}\text{C}$  or not.

As the testing device and the whole procedure have proven its precision and practicability, further testing devices are being constructed and calibrated. Round robin tests in different European geotechnical laboratories commenced. These tests will underpin the reproducibility and independency of the testing procedure. Thus the general conditions for a comprehensive quality assurance of frost-resistant grouting material will be provided.

## ACKNOWLEDGMENTS

The writers would like to thank the State Ministry for Urban Development and the Environment Hamburg Germany for their help. Also we would like to thank Wolfram Rühak for his suggestions to the numerical implementation.

## References

- Allan, M. L., 2000, "Materials Characterization of Superplasticized Cement-Sand Grout," *Cem. Concr. Res.*, Vol. 30, pp. 937-942.
- Allan, M. L. and Philippacopoulos, A. J., 1998, "Thermal Conductive Cementitious Grouts for Geothermal Heat Pumps: Progress Report FY 98," *BNL-66103*, Informal Report, Brookhaven National Laboratory, Upton, NY.

- Anbergen, H., Frank, J., Müller, L. and Sass, I., 2013, "Entwicklung eines Einheitlichen Prüfverfahrens für den Nachweis der Frost-Tau-Wechselwiderstandsfähigkeit von Verpressmaterial," *Proceedings of the German Heat Pump Association (BWP)*—Praxisforum Offenburg, Germany.
- Anbergen, H. and Sass, I., 2013, "Freeze-Thaw-Behaviour: Observations in Grouted Borehole Heat Exchangers," *Proceedings of the Thirty-Eighth Workshop on Geothermal Reservoir Engineering*, Stanford Univ., Stanford, CA.
- ASTM D-5084-10, 2010: Standard Test Methods for Measurement of Hydraulic Conductivity of Saturated Porous Materials Using a Flexible Wall Permeameter, *Annual Book of ASTM Standards*, ASTM International, West Conshohocken, PA.
- ASTM D-6035-08, 2008: Standard Test Methods for Determining the Effect of Freeze-Thaw on Hydraulic Conductivity of Compacted or intact Soil Specimens Using a Flexible Wall Permeameter *Annual Book of ASTM Standards*, ASTM International, West Conshohocken, PA.
- Bassetti, S., Rohner, E., Signorelli, S. and Matthey, B., 2006, "Dokumentation von Schadensfällen bei Erdwärmesonden—Schlussbericht," *Geothermie Report 99995*, Swiss Federal Office of Energy, Switzerland.
- Baumann, K., Niehues, B., Tholen, M. and Treskatis, C., 2003, "Untersuchungen zur Bestimmung von Qualitätskriterien für Abdichtungsmaterialien im Brunnenbau," *Final Report*, DVGW, Bonn, Germany.
- Bronfenbrener, L. and Bronfenbrener, R., "Modeling Frost Heave in Freezing Soils," *Cold Regions Sci. Technol.*, Vol. 61, 2010, pp. 43–64.
- Carlsaw, H. S. and Jaeger, J. C., 1959, *Conduction of Heat in Solids*, 2nd ed., Oxford University, Press, Oxford, UK.
- CEN ISO/TS 17892-11:2004, 2005: Geotechnical Investigation and Testing Laboratory Testing of Soil Part 11: Determination of Permeability by Constant and Falling Head, Deutsches Institut für Normung, Beuth-Verlag, Berlin.
- CEN-TS 14418:2005, 2006: Geosynthetic Barriers—Test Method for the Determination of the Influence of Freezing—Thawing Cycles on the Permeability of Clay Geosynthetic Barriers, Deutsches Institut für Normung, Beuth-Verlag, Berlin.
- Coussy, O., 2005, "Poromechanics of Freezing Materials," *J. Mech. Phys. Solids*, Vol. 53, pp. 1689–1718.
- EN 1367-1:2007, 2007: Tests for Thermal and Weathering Properties of Aggregates—Part 1: Determination of Resistance to Freezing and Thawing, Deutsches Institut für Normung, Beuth-Verlag, Berlin, Germany.
- Konrad, J.-M. and Morgenstern, N. R., 1980, "A Mechanistic Theory of Ice Lens Formation in Fine-Grained Soils," *Can. Geotech. J.*, Vol. 17, pp. 473–486.
- Mehnert, E., 2004, "The Environmental Effects of Ground-Source Heat Pumps—A Preliminary Overview," *Open-File Series Report 2004-2*, Illinois State Geological Survey, University of Illinois at Urbana-Champaign, Champaign, IL.
- Moo-Young, H. K. and Zimmie, T. F., 1996, "Geotechnical Properties of Paper Mill Sludges for Use in Landfill Covers," *J. Geotech. Eng.*, Vol. 122, pp. 768–775.
- Ono, T., 2002, "Lateral Deformation of Freezing Clay Under Triaxial Stress Condition Using Laser-Measuring Device," *Cold Regions Sci. Technol.*, Vol. 35, pp. 45–54.
- Philippacopoulos, A. J. and Berndt, M. L., 2001, "Influence of Debonding in Ground Heat Exchangers Used With Geothermal Heat Pumps," *Geothermics*, Vol. 30, pp. 527–545.
- Rühaak, W. and Sass, I., 2013, "Applied Thermo-Hydro-Mechanical Coupled Modeling of Geothermal Prospection in the Northern Oberrheingraben," *Proceedings of the Thirty-Eighth Workshop on Geothermal Reservoir Engineering*, Stanford University, Stanford, CA.
- Sass, I. and Lehr, C., 2011, "Improvements on the Thermal Response Test Evaluation Applying the Cylinder Source Theory," *Proceedings of the Thirty-Sixth Workshop on Geothermal Reservoir Engineering*, Stanford University, Stanford, CA.
- Sugama, T., 2006, "Advanced Cements for Geothermal Wells," *BNL-77901-2007-IR*, Brookhaven National Laboratory, Upton, NY.
- Unold, F., 2006, "Der Gefriersog bei der Durchfrostung und das Kompressionsverhalten des wieder aufgetauten Bodens," Ph.D. thesis, Universität der Bundeswehr, München, Germany.
- VDI, Ed., 2001, VDI-Guideline 4640 Part 2: *Thermal Use of the Underground—Ground Source Heat Pump Systems*, Beuth, Berlin.